BIOCHEMISTRY
including biophysical chemistry & molecular biology

Article

pubs.acs.org/biochemistry

Membranotropic Regions of the Dengue Virus prM Protein

Henrique Nemésio and José Villalaín*

Instituto de Biología Molecular y Celular, Universidad "Miguel Hernández", E-03202 Elche-Alicante, Spain

Supporting Information

ABSTRACT: The Dengue virus (DENV) prM protein consists of two moieties, the pr and M domains. Apart from preventing the premature fusion activity of the DENV E protein, prM has several other unknown biological roles, displaying both protein−protein and membrane−protein interactions. Although the prM protein is an essential component of the DENV viral cycle, little is known about its biological functions and what regions of this protein are responsible for said functions. By performing an exhaustive study of membrane rupture induced by a prM peptide library on simple and complex model membranes as well as their ability to modulate the phospholipid phase transitions of 1,2-dimyristoyl-*sn*-glycero-3-phosphatidylcholine and 1,2-dimyristoyl-*sn*-glycero-3-[phospho-*rac*-glycerol], we identified six membranotropic regions on the prM protein. Apart from the previously identified two transmembrane segments of the protein, one of these regions probably interacts with the fusion E protein and another one, the stem segment, would interact with the membrane modulating its structure. These data will help us understand the molecular mechanism of viral entry and morphogenesis, allow the identification of new targets for the treatment of Dengue virus infection, and make possible the future development of DENV entry inhibitors.

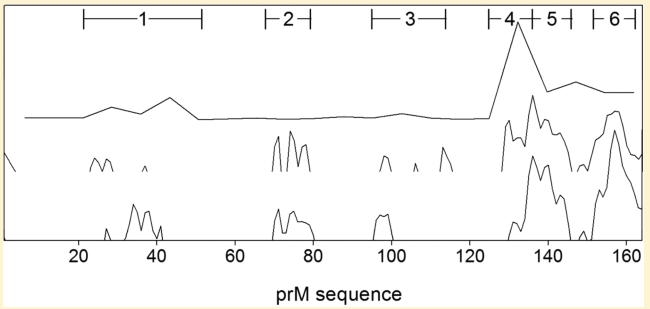

Dengue virus (DENV) is a constituent of the genus *Flavivirus*, which along with *Hepacivirus* and *Pestivirus* composes the Flaviviridae family.[1−3] Dengue disease is becoming a great public health concern because DENV is the arthropod-borne virus with the highest incidence in the human population, with >390 million estimated infections per year.[4] Patients infected can show a wide range of symptoms, from less to most severe: asymptomatic, mild fever (Dengue fever), Dengue hemorrhagic fever, and Dengue shock syndrome.[5] The two latter life-threatening serious conditions are often but not always developed in individuals secondarily affected by heterologous subtypes. There is actually no clinical treatment for DENV infection, and no antivirals or vaccines against DENV are currently available; therefore, more than 2 billion people, mainly in poor countries, are at risk in the world.[6] The main strategy for thwarting the spread of the infection is based on the control of the mosquito vector (*Aedes* spp.) itself, but the ever-increasing global temperature and traveling frequency introduce a real risk of the vector spreading to previously unaffected zones.

DENV is a positive-sense, single-stranded RNA virus of approximately 10.7 kb. It contains untranslated regions at the 5′ and 3′ ends, flanking a single open reading frame encoding a polyprotein of >3000 amino acids, which after infection is subsequently cleaved by cellular and viral proteases into three structural proteins (C, prM, and E), and seven nonstructural proteins.[7] The surface of the virion is composed of a lipid bilayer in which 180 copies of E and M protein (a derivative of the prM protein) heterodimers are embedded. The nucleocapsid (composed of C protein and viral RNA) is inside this lipid bilayer.[7] Like other enveloped viruses, the DENV enters the cells through receptor-mediated endocytosis in a rather complicated process[3,7−9] and rearranges cell internal membranes to establish the replication complex (membranous web).[10−12] Details about the DENV replication process remain largely unclear, but most if not all of the DENV proteins are involved and function in a complex web of protein−protein interactions.[3,7] DENV replicates its genome in a membrane-associated replication complex, and morphogenesis and virion budding have been suggested to take place in the endoplasmic reticulum (ER) or ER-derived membranes. Considering the structural proteins, the C protein plays a role in the specific encapsidation of the genome and is essential for viral assembly.[13] The E protein is a class II fusion protein, essential for attachment, membrane fusion, and assembly. A series of conformational changes occurring in the DENV E protein, driven by the endosomal low pH, lead to the fusion of the viral and endosomal membranes.[3,7] The stem region of the E protein has been proposed to be engaged in the fusion process, but the critical regions of the stem region are not known with certainty.[7−9,14]

The prM protein consists of an N-terminal pr domain followed by the M protein separated by a furin cleavage site.[15] The pr part of the protein consists mainly of β-strands, whereas

Received: June 11, 2014
Revised: July 30, 2014
Published: July 30, 2014

dx.doi.org/10.1021/bi500724k | *Biochemistry* 2014, 53, 5280−5289

Table 1. Sequences and Residue Positions of All Peptides Contained in the DENV2 NGC prM-Derived Library

peptide number	no. of amino acids	sequence	amino acid positions	net charge
1	16	FHLTTRNGEPHMIVSR	1−16	+1
2	18	NGEPHMIVSRQEKGKSLL	7−24	+1
3	17	SRQEKGKSLLFKTEDGV	15−31	+1
4	18	SLLFKTEDGVNMCTLMAM	22−39	−1
5	15	GVNMCTLMAMDLGEL	30−44	−2
6	18	TLMAMDLGELCEDTITYK	35−52	−3
7	15	ELCEDTITYKCPFLK	43−57	−1
8	17	TITYKCPFLKQNEPEDI	48−64	−1
9	20	FLKQNEPEDIDCWCNSTSTW	55−74	−3
10	18	DCWCNSTSTWVTYGTCTT	63−80	−1
11	18	TWVTYGTCTTTGEHRREK	71−88	+1
12	18	TTTGEHRREKRSVALVPH	79−96	+2
13	18	EKRSVALVPHVGMGLETR	87−104	+1
14	15	PHVGMGLETRTETWM	95−109	−1
15	18	GLETRTETWMSSEGAWKH	100−117	−1
16	18	WMSSEGAWKHAQRIETWI	108−125	0
17	18	KHAQRIETWILRHPGFTI	116−133	+2
18	17	WILRHPGFTIMAAILAY	124−140	+1
19	17	FTIMAAILAYTIGTTHF	131−147	0
20	18	LAYTIGTTHFQRALIFIL	138−155	+1
21	19	HFQRALIFILLTAVAPSMT	146−164	1

the M portion consists of a linear structure followed by a mainly α-helical stem region and two transmembrane helices.[15] During maturation of the viral particle in the host cell, after it has traversed the trans Golgi network, the decreasing pH inside the vesicle containing the viral particle(s) (with E and prM proteins embedded in its lipid bilayer) induces a conformational change in this complex that is reversible as long as prM remains intact.[15] As soon as furin cleaves the bond between pr and M, the former is released and the conformational change is no longer reversible, rendering the virus fully mature and, thus, infectious.[7,15] The M protein remains in the mature particle as a transmembrane protein covered by the E protein layer. Some nonstructural functions have been also assigned to prM, including a role in apoptosis, because a region of the M protein triggered apoptosis in mouse neuroblastoma and human hepatoma cells.[16] It has also been shown that prM/M interacts with host proteins such as human dynein, vacuolar ATPase, and claudin 1, facts that support its importance in the entry and assembly stages of the viral cycle.[17−20] It has been reported that the expression of M protein alone was sufficient for it to adopt the predicted topology and localize to the ER membrane and that the pr peptide might contain an ER retention signal, possibly important for the correct formation of the prM−E complexes.[21] Interestingly, Zhang et al. have described protein M as a membrane-anchored, pH-sensing, multistep chaperone of protein E.[22] Despite these very important results, the full impact of prM/M in the viral cycle is far from defined.

We have recently identified the membrane-active regions of a number of viral proteins by observing the effect of protein-derived peptide libraries on model membrane integrity.[23−28] These results allowed us to propose the location of different protein segments implicated in either protein−lipid or protein−protein interactions and help us to understand the mechanisms underlying the interaction between viral proteins and membranes. Motivated by the need to understand the interaction of prM with membranes, considering that it is essential in the viral RNA replication process and, additionally, that DENV protein−membrane and protein−protein interactions are an attractive target for antiviral drug development, we have characterized the membranotropic regions of the DENV prM protein. By using a peptide library encompassing the full length of prM and assessing their effect on membrane integrity using model biomembranes, we have identified several prM regions with different interacting capabilities. These data will help us understand the molecular mechanism of viral fusion and morphogenesis, identify new targets for the treatment of Dengue virus infection, and make possible the future development of DENV entry inhibitors that may lead to new vaccine strategies.

MATERIALS AND METHODS

Materials and Reagents. The peptide library derived from DENV type 2 NGC prM protein, consisting of 21 peptides (Table 1), was obtained from BEI Resources (National Institute of Allergy and Infectious Diseases, Manassas, VA). All peptides had a purity of ∼80% and were not capped. Peptides were solubilized in a water/2,2,2-trifluoroethanol mixture at 70:30 ratios (v/v). Bovine brain phosphatidylserine (BPS), bovine liver L-α-phosphatidylinositol (BPI), cholesterol (Chol), egg L-α-phosphatidic acid (EPA), egg L-α-phosphatidylcholine (EPC), egg sphingomyelin (ESM), egg transphosphatidylated L-α-phosphatidylethanolamine (TPE), bovine heart cardiolipin (CL), 1,2-dimyristoyl-*sn*-glycero-3-phosphatidylcholine (DMPC), 1,2-dimyristoylphosphatidylglycerol (DMPG), 1,2-dielaidoyl-*sn*-glycero-3-phosphatidylethanolamine (DEPE), and liver lipid extract were obtained from Avanti Polar Lipids (Alabaster, AL). The synthetic endoplasmic reticulum (ER) mixture had a 59:0.37:7.7:18:3.1:1.2:3.4:7.8 EPC:CL:BPI:TPE:BPS:EPA:ESM:Chol lipid composition,[29,30] whereas the liver lipid extract contained 42% phosphatidylcholine, 22% phosphatidylethanolamine, 7% Chol, 8% phosphatidylinositol, 1% lysophosphatidylinositol, and 21% miscellaneous lipids, including neutral ones, as stated by the manufacturer. 1,6-Diphenyl-1,3,5-hexatriene (DPH) was obtained from Molecular Probes (Eugene, OR). 5-Carboxyfluor-

dx.doi.org/10.1021/bi500724k | *Biochemistry* 2014, 53, 5280−5289

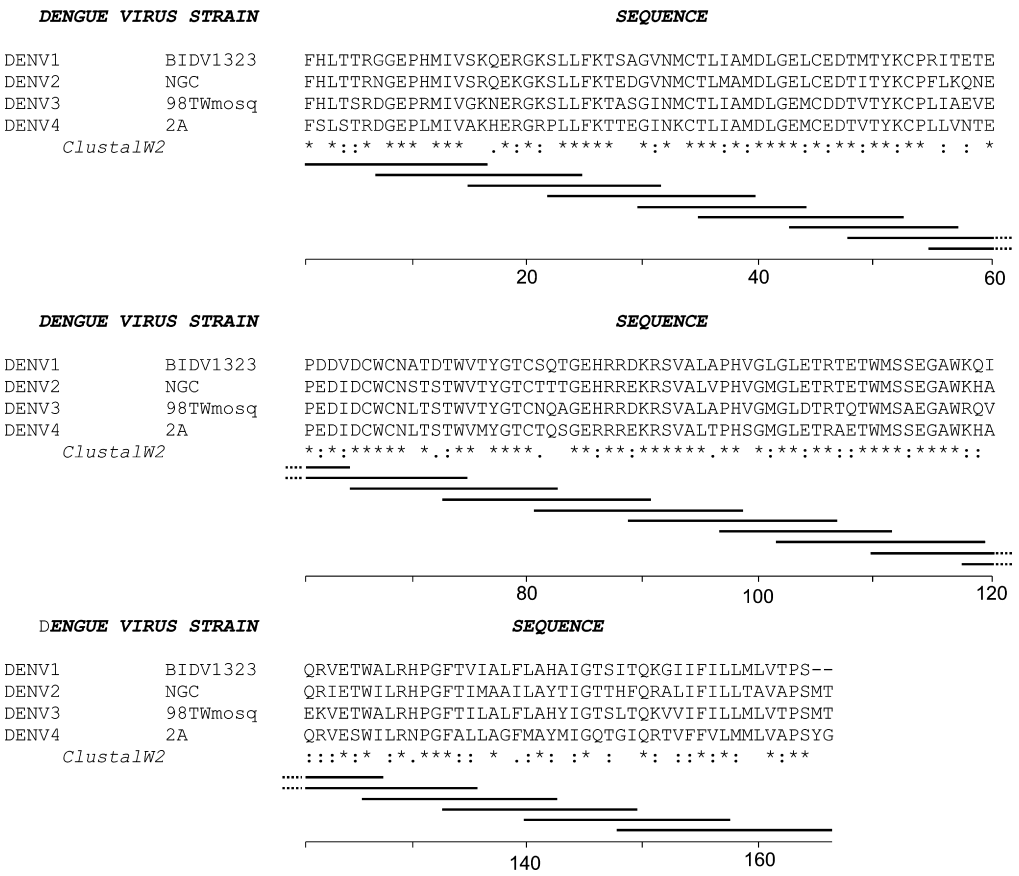

Figure 1. Sequences of the prM protein for four representative different DENV serotypes. The sequences were split for better visualization. A global Clustalw2 alignment was computed using 41 strains derived from DENV1 (02_20, 05K4147DK1, 297arg00, BIDV1323, BIDV1800, BIDV1841, BIDV1926VN2008, BIDV2143, BIDV2243VE2007, and ThD1004901), DENV2 (NGC, BIDV633, BIDV687, CSF381, CSF63, DakArD20761, DF707, DF755, MD1504, MD903, and MD917), DENV3 (05K797DK1, 07CHLS001, 98, 98TWmosq, BIDV1831VN2007, BIDV1874VN2007, BR29002, C036094, TB55i, and ThD31283_98), and DENV4 (2A, BIDV2165VE1998, BIDV2170VE1999, H241, rDEN4del30, Sin897695, ThD4047697, ThD4048501, Vp4, and Yama). Below each table there is a graphic line showing the relative location and length of each peptide in the peptide library. The maximal overlap between adjacent peptides is 11 amino acids.

escein (CF, >95% by high-performance liquid chromatography), Triton X-100, EDTA, and HEPES were purchased from Sigma-Aldrich (Madrid, Spain). All other chemicals were commercial samples of the highest purity available (Sigma-Aldrich). Water was deionized, distilled twice, and passed through Milli-Q equipment (Millipore Ibérica, Madrid, Spain) to a resistivity of >18 MΩ cm.

Vesicle Preparation. Aliquots containing the appropriate amount of lipid in a chloroform/methanol mixture [2:1 (v/v)] were placed in a test tube; the solvents were removed by evaporation under a stream of O_2-free nitrogen, and finally, traces of solvents were eliminated under vacuum in the dark for >3 h. The lipid films were resuspended in an appropriate buffer and incubated at either 25 or 10 °C above the phase transition temperature (T_m) with intermittent vortexing for 30 min to hydrate the samples and obtain multilamellar vesicles (MLVs). The samples were frozen and thawed five times to ensure complete homogenization and maximization of peptide−lipid contacts with occasional vortexing. Phospholipid and peptide concentrations were measured by methods described previously.[31,32]

Membrane Leakage Measurement. Large unilamellar vesicles (LUVs) with a mean diameter of 0.1 μm were prepared from MLVs by the extrusion method[33] using polycarbonate filters with a pore size of 0.1 μm (Nuclepore Corp., Cambridge, CA) in buffer containing 10 mM Tris, 20 mM NaCl (pH 7.4, 25 °C), and CF at a concentration of 40 mM. Breakdown of the vesicle membrane leads to the leakage of its contents, i.e., CF fluorescence. Nonencapsulated CF was separated from the vesicle suspension through a Sephadex G-75 filtration column (Pharmacia, Uppsala, Sweden) eluted with buffer containing 10 mM Tris, 100 mM NaCl, and 0.1 mM EDTA (pH 7.4). The leakage of intraliposomal CF was assayed by treating the probe-loaded liposomes (final lipid concentration of 0.125 mM) with the appropriate amounts of peptides on microtiter plates stabilized at 25 °C using a microplate reader (FLUOstar, BMG Labtech), each well containing a final volume of 170 μL. The medium in the microtiter plates was continuously stirred to allow the rapid mixing of the peptide and vesicles. Leakage was measured at an approximate peptide:lipid molar ratio of 1:25. Changes in fluorescence intensity were recorded with excitation and emission wavelengths set at 492 and 517 nm, respectively. One hundred percent release was achieved by adding Triton X-100 to a final concentration of 0.5% (w/w) to the microtiter plates. Fluorescence measurements were made initially with probe-loaded liposomes, then by adding a peptide solution, and finally byy adding Triton X-100 to produce 100% leakage. Leakage was quantified on a percentage basis according to the equation % release = $[(F_f - F_0)/(F_{100} - F_0)] \times 100$, F_f being the equilibrium value of fluorescence after peptide addition, F_0

dx.doi.org/10.1021/bi500724k | Biochemistry 2014, 53, 5280−5289

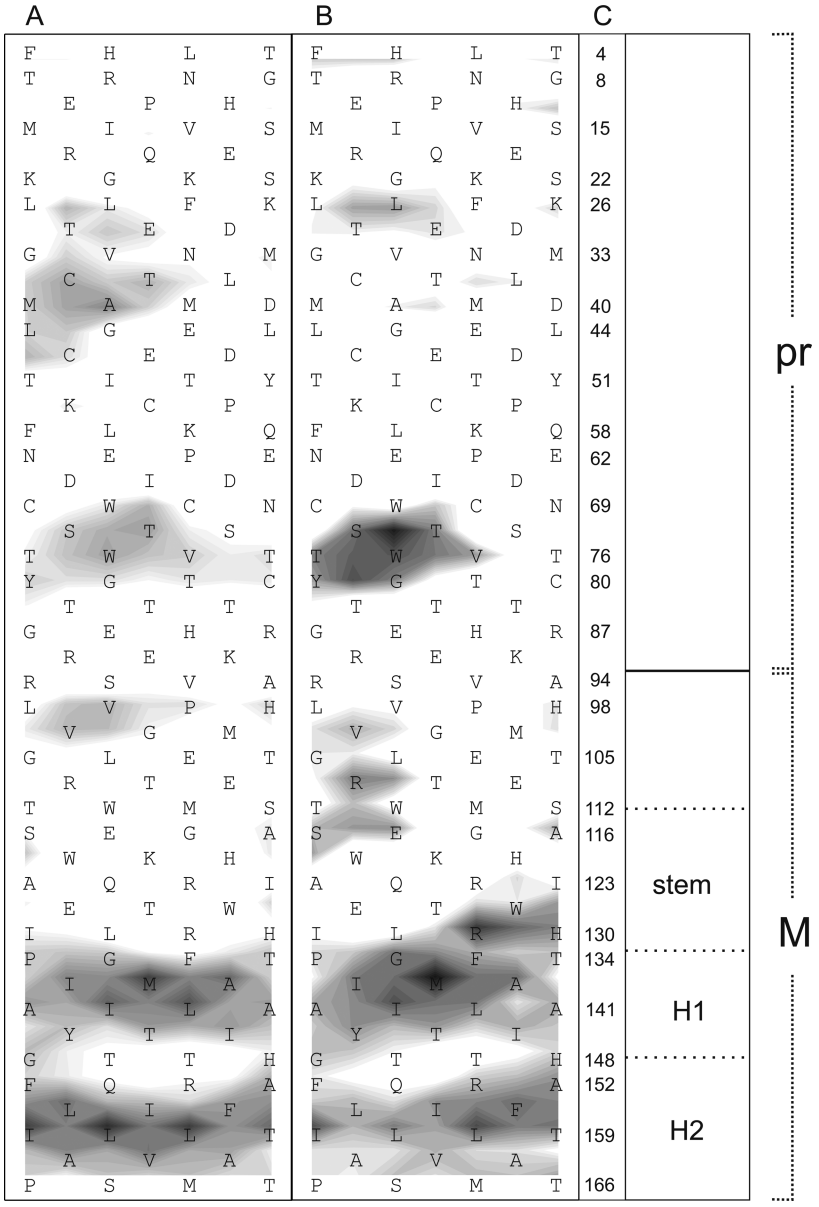

Figure 2. Calculated two-dimensional plot of the average normalized (A) water to membrane and (B) water to interface transfer free energy scales in kilocalories per mole for the prM protein.[41] Transfer free energies were obtained from refs 42−47. Positive values represent positive transfer free energy values, and therefore the higher (darker) the value, the greater the probability of interacting with the membrane surface and/or hydrophobic core. The sequence of the DENV2 NGC prM protein overlaps the two-dimensional plots to easily follow the text. The sequence number of the rightmost residue and a schematic diagram of the different domains of the prM protein according to literature are shown in panel C.

the initial fluorescence of the vesicle suspension, and F_{100} the fluorescence after the addition of Triton X-100. For details, see refs 34 and 35.

Differential Scanning Calorimetry. MLVs were formed as stated above in 20 mM HEPES, 100 mM NaCl, and 0.1 mM EDTA (pH 7.4). The peptide was added to obtain a peptide:lipid molar ratio of 1:15. The final volume was 0.8 mL (lipid concentration of 0.6 mM), which was incubated 10 °C above the T_m of each phospholipid for 1 h with occasional vortexing. Differential scanning calorimetry (DSC) experiments were performed in a VP-DSC differential scanning calorimeter (MicroCal LLC) under a constant external pressure of 30 psi to prevent the formation of bubbles, and samples were heated at a constant scan rate of 60 °C/h. Experimental data were corrected from small mismatches between the two cells by subtracting a buffer baseline prior to data analysis. The excess heat capacity functions were analyzed using Origin 7.0 (Microcal Software). The thermograms were defined by the onset and completion temperatures of the transition peaks obtained from heating scans. To avoid artifacts due to the thermal history of the sample, the first scan was never considered; second and additional scans were conducted until a reproducible and reversible pattern was obtained.

Steady-State Fluorescence Anisotropy. MLVs were formed in a buffer composed of 100 mM NaCl, 0.1 mM EDTA, and 20 mM HEPES at pH 7.4 or 6.0 (at 25 °C). Aliquots of DPH in *N*,*N*′-dimethylformamide (0.2 mM) were directly added to the lipid suspension to obtain a probe:lipid molar ratio of 1:500. DPH, a widespread membrane fluorescent probe for monitoring the organization and dynamics of membranes, is known to partition mainly into the hydrophobic core of the membrane.[36] Samples were incubated for 60 min 10

dx.doi.org/10.1021/bi500724k | *Biochemistry* 2014, 53, 5280−5289

°C above the gel to liquid-crystalline phase transition temperature T_m of the phospholipid mixture. Afterward, the peptides were added to obtain a peptide:lipid molar ratio of 1:15 and incubated 10 °C above the T_m of each lipid for 1 h, with occasional vortexing. All fluorescence studies were conducted using 5 mm × 5 mm quartz cuvettes in a final volume of 400 μL (lipid concentration of 315 μM). The steady-state fluorescence anisotropy was measured with an automated polarization accessory using a Varian Cary Eclipse fluorescence spectrometer, coupled to a Peltier for automatic temperature change. The vertically and horizontally polarized emission intensities, elicited by vertically polarized excitation, were corrected for background scattering by subtracting the corresponding polarized intensities of a phospholipid preparation lacking probes. The G factor, accounting for differential polarization sensitivity, was determined by measuring the polarized components of the fluorescence of the probe with horizontally polarized excitation ($G = I_{HV}/I_{HH}$). Samples were excited at 360 nm, and emission was recorded at 430 nm, with excitation and emission slits of 5 nm. Anisotropy values were calculated using the formula $\langle r \rangle = (I_{VV} - GI_{VH})/(I_{VV} + 2GI_{VH})$, where I_{VV} and I_{VH} are the measured fluorescence intensities (after appropriate background subtraction) with the excitation polarizer vertically oriented and the emission polarizer vertically and horizontally oriented, respectively.

RESULTS AND DISCUSSION

We have conducted an exhaustive analysis of the different regions of the DENV prM protein that might interact either with phospholipid membranes or with other proteins using an approach similar to that used previously,[27,28] i.e., using a peptide library derived from the prM protein (Table 1). Although we have studied the effect of a prM peptide library derived from the DENV2 strain, the information gathered should be similar for the other three DENV strains because there is a remarkable identity at the primary structure level of the protein for the four known DENV strains (Figure 1). Figure 1 shows the sequences of the prM protein for four representative different DENV serotypes and the alignment of 41 different strains pertaining to the four serotypes. If we consider only fully conserved residues, the level of sequence identity is 53%, but considering conserved and strongly similar residues, the level of identity increases to 78%. The peptide library we have used in this work is composed of 21 different peptides (Table 1), and their correlation with the prM sequence is shown in Figure 1. Because the peptide library includes the whole sequence of the protein and each individual peptide, i, overlaps with two and three consecutive peptides, $i + 1$ and $i + 2$, by approximately 11 and 4 residues, respectively, the obtained data can be extrapolated to protein segments rather than on the effect of isolated peptides. Apart from its availability and peptide solubility, this is the main reason to choose this peptide library.

Two-dimensional plots of hydrophobicity and interfaciality for the whole prM protein, depicted in Figure 2, were obtained taking into consideration the arrangement of the amino acids in the space assuming it adopts an α-helical structure along the whole sequence; they were used to detect surfaces along the prM protein that might be identified as membrane and/or protein interacting zones.[24,37] As observed in Figure 2, we can recognize the presence of different regions with large hydrophobic moment values along the surface of the protein. Using these two-dimensional plots, it is possible to distinguish two types of patches, those that do not comprise the perimeter of the helix and those that embrace the full perimeter.[37] The first type could favor the interaction with other similar patches along the same or other proteins as well as with the membrane surface, whereas the second could represent transmembrane domains or membrane interacting domains.[23,25,37,38] As shown in Figure 2, two patches corresponding to the first type and two patches corresponding to the second type are clearly observed; the first two would correspond approximately to residues 66−80 and 122−131, whereas the other two would correspond approximately to residues 133−144 and 152−162. Residues 66−80 pertain to the pr moiety, whereas residues 122−131, 133−144, and 152−162 pertain to the M moiety.[15] The patch located between residues 66 and 80 of pr, which is more intense on the water to interface than on the water to bilayer map, is close to the electrostatic patch of the pr protein comprising residues Asp^{63} and Asp^{65} that specifically interacts with another DENV E protein electrostatic patch (residues His^{244} and Lys^{247}).[15] The existence of an interfacial/hydrophobic patch near an electrostatic one would imply that both of them would interact with complementary patches located on the DENV E protein surface.[15,39] With respect to the M protein, residues 122−131, 133−144, and 152−162 pertain to the stem/interfacial and transmembrane regions of the M protein. This is in accordance with previously published data that showed that the stem region was defined from residue 111 to 131 and the two mainly α-helical transmembrane helices went from residue 131 to 166.[15] This description of interfacially and hydrophobically rich surfaces fits very well with previously published data for the prM protein and adds interesting information highlighting the great utility of these two-dimensional maps in identifying specific regions in proteins.[24,37]

We have studied the effect of the prM peptide library on membrane rupture by monitoring the leakage of CF from different liposome compositions, and the results are presented in Figure 3.[38] We have tested five different lipid compositions, simple and complex (Figure 3). The simple compositions contained EPC and Chol at a phospholipid molar ratio of 5:1 (Figure 3A), EPC and SM at a phospholipid molar ratio of 5:1 (Figure 3B), and EPC, SM, and Chol at a phospholipid molar ratio of 5:1:1 (Figure 3C), whereas the complex ones consisted of an ER synthetic lipid mixture resembling the ER membrane (Figure 3D) and a lipid extract of liver membranes (Figure 3E). It should be recalled that DENV is associated with membranes of the ER or an ER-derived modified compartment. The leakage data (Figure 3A−E) show that some peptides exerted a significant leakage effect, most probably by giving rise to local defects in the membrane. Although there were some differences depending on liposome composition, they were not sufficiently significant to infer any specific relationship between lipid composition and leakage. The leakage effects were mainly focused on two specific regions delimited by peptides 4−6 (residues 22−52) and 18−21 (residues 124−164), the first group pertaining to the pr moiety and the second to the M moiety. Leakage values elicited by peptides 18−21 were significant, because they oscillated between 30 and 50%. Lower, but significant, leakage values were found for peptides 4−6, because 10−15% leakage values were found (Figure 3).

The average leakage of all membrane compositions tested for the prM protein is presented in Figure 3F and can be compared to the water to interfacial (Figure 3G; data obtained from Figure 2A) and water to bilayer data (Figure 3H; data obtained from Figure 2B). It can be observed that the leakage data fit

dx.doi.org/10.1021/bi500724k | Biochemistry 2014, 53, 5280−5289

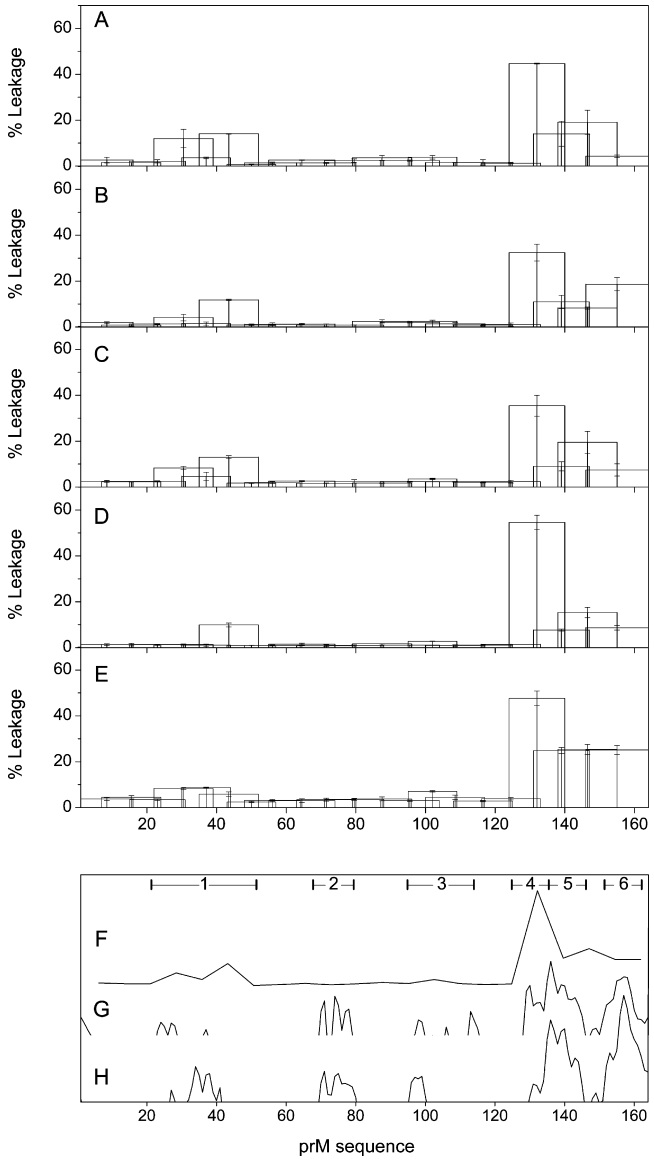

Figure 3. Effect of the peptide library derived from the DENV2 prM protein on the release of LUV CF contents for different lipid compositions. Leakage data (membrane rupture) for LUVs composed of (A) EPC and Chol at a phospholipid molar ratio of 5:1, (B) EPC and SM at a phospholipid molar ratio of 5:1, and (C) EPC, SM, and Chol at a phospholipid molar ratio of 5:1:1, (D) the ER complex synthetic lipid mixture, and (E) the lipid extract of liver membranes. Vertical bars indicate standard deviations of the mean of quintuplicate samples.

perfectly well with the hydrophobic and interfacial regions, overall defining six different and characteristic regions (Figure 3F). Region 1 would be a broad region and comprise residues 20−50; this region would be defined by relatively low leakage and hydrophobic values. Region 2 would be defined by residues 70−80 and would be characterized by a relatively high interfacial and hydrophobic character but no leakage. In principle, this region would define a protein−protein interaction domain. Region 3, comprised by residues 95 and 115, would be defined by no leakage and low interfacial and hydrophobic character, which might suggest a weak protein−protein interacting region. Region 4 would be defined by significant and dramatic leakage values concurrent with high interfaciality and low hydrophobicity. This region would outline the stem/pretransmembrane region of the prM protein. The existence of pretransmembrane domains in viral proteins with a strong propensity for partitioning into membrane interfaces is well-known.[40] These domains are characterized by having high water to interface transfer free energies immediately followed by high water to bilayer transfer free energies, usually with some overlap. These characteristics are exhibited by prM region 4 (see Figure 3G,H), so that it would be reasonable to suppose that the stem region of the prM protein could behave as a pretransmembrane interacting domain. Regions 5 and 6 would be defined by residues 130−142 and residues 149−162, respectively, and present high leakage and significant interfacial and hydrophobic values, delineating the extension of the two transmembrane domains of the prM protein. In summary, peptides from the DENV2 prM protein, capable of inducing membrane leakage, did not have any specific interaction with any specific lipid, as they elicited similar membrane rupture on all types of membrane model systems in a manner independent of phospholipid headgroup, charge, or structure. The coincidental results obtained through both the theoretical and experimental data would point out that these sequences should be important regions of this protein and would be engaged in membrane interaction with either its surface or its interior.

Phospholipids can undergo a cooperative melting reaction linked to the loss of conformational order of the lipid chains; this melting process can be influenced by many types of molecules, including peptides and proteins. The effect of the prM peptide library on the thermotropic phase behavior of phospholipid multilamellar vesicles was studied using differential scanning calorimetry (DSC) (Figure 4). Aqueous dispersions of the pure phospholipids DMPC and DMPG undergo a gel to liquid-crystalline phase transition ($P_{\beta'}-L_{\alpha}$) at a T_m in the lamellar phase of approximately 23−24 °C and in addition a pretransition at approximately 12−13 °C ($L_{\beta'}-P_{\beta'}$). As shown in Figure 4A, when DMPC was studied in the presence of each of the peptides corresponding to the prM-derived peptide library, both pre and main transitions were present in all samples, displaying similar enthalpies, in a manner independent of the peptide tested. There were minor changes in the T_m values for several samples (peptides 12 and 14 induced the strongest effect because they decreased the T_m from 23.4 °C in the pure phospholipid to 22 °C in the presence of the peptides). There was also some decrease in the cooperativity of DMPC upon addition of the peptide, but similarly to what has been mentioned above, the increase in width was slight. Contrary to what was seen in DMPC in the case of the negatively charged phospholipid DMPG, some peptides elicited a significant effect on the pre and main transition temperatures (Figure 4B). The most significant effect was observed for peptides 16 [net charge of 0 (see Table 1)] and 17 (net charge of +2), because they abolished the pretransition and significantly decreased the cooperativity of the main transition (see Figure 4). These peptides increased the T_m of DMPC from 22.8 °C in the pure phospholipid to 25.6 °C in the presence of the peptides. Peptides 8 and 11, having net charges of −1 and +1, respectively, also elicited a significant effect on DMPG, because they induced the appearance of more than one peak and an increase of approximately 4−5 °C in the width of the T_m transition (Figure 4). Besides peptides 8 and 11, peptides 1 and 18−21 (net charges of +1, +1, 0, +1, and +1, respectively) also induced significant effects on the T_m transition of DMPG, because they were responsible for the

dx.doi.org/10.1021/bi500724k | *Biochemistry* 2014, 53, 5280−5289

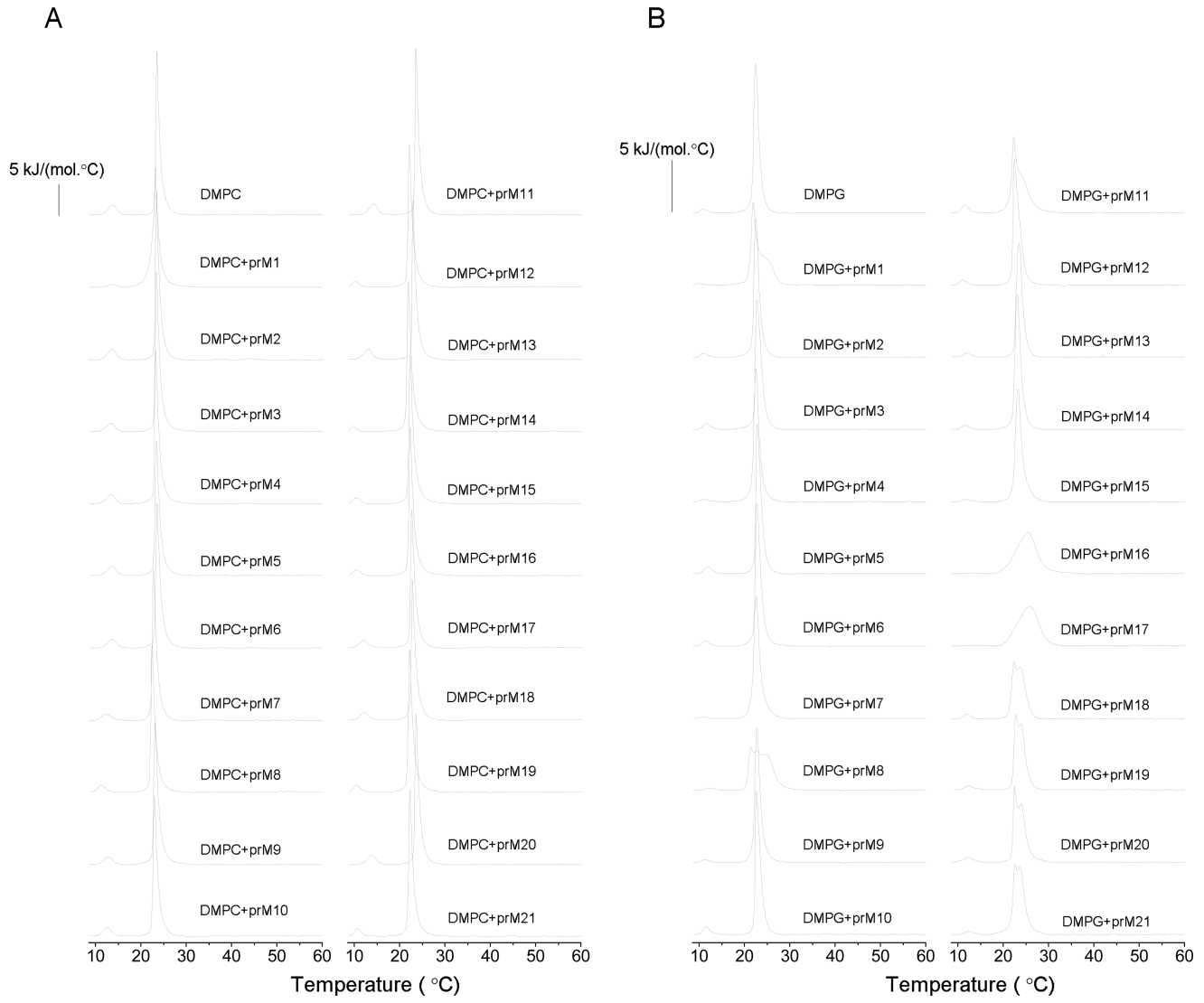

Figure 4. Differential scanning calorimetry heating thermograms corresponding to model membranes composed of (A) DMPC and (B) DMPG in the absence and presence of the peptides belonging to the prM protein library at a phospholipid:peptide molar ratio of 10:1. All the thermograms were normalized to the same amount of lipid.

appearance of two peaks in the main transition (Figure 4B). The presence of different peaks in the thermograms indicates that the peptides were capable of affecting DMPG model membranes inducing the formation of mixed lipid phases, enriched and impoverished in peptide. Via comparison of Figures 3 and 4, it can be observed that there is a coincidence of the high-effect peptides with high-leakage zones, demonstrating their specific interaction with the membrane as well as their modulatory effect. The specific effect that some peptides have on DMPG does not seem to be exclusively electrostatic, because the net charges of those peptides affecting more dramatically the phospholipid (see above) range from −1 to +2, including the intermediate values.

The effect of the prM peptide library on the structural and thermotropic properties of phospholipid membranes was also investigated by measuring the steady-state fluorescence anisotropy of the fluorescent probe DPH incorporated into model membranes as a function of temperature. The phospholipids that have been studied are DMPC at pH 7.4 and 6.0 (Figures 1 and 2 of the Supporting Information, respectively) and DMPG at pH 7.4 (Figure 5). DMPC, in the presence of several of the peptides and at both pH values, presented a slight decrease in the cooperativity of the thermal transition, but no significant change in the T_m when compared to that of the pure lipid (Figures 1 and 2 of the Supporting Information). However, there were several peptides that increased the anisotropy of DMPC above the T_m of the phospholipid, specifically peptides 4, 5, and 18−21 (Figures 1 and 2 of the Supporting Information). The increase in anisotropy elicited by peptides 18−21 was significantly higher than that observed for peptides 4 and 5. It should be recalled that peptides 4 and 5 pertain to region 1 and peptides 18−21 to regions 4−6 as defined previously (Figure 3). A relatively similar pattern was found for DMPG, because some peptides decreased slightly the cooperativity of the thermal transition without altering the T_m itself (Figure 5). Like what has been mentioned above, peptides 4, 5, and 18−21 increased the anisotropy of the mixture above but not below the T_m of the phospholipid, significantly higher for the later than for the former (Figure 5). Interestingly, these data would suggest that peptides 4 and 5 interact with the membrane interface and peptides 18−21, which interestingly coincide with the two

dx.doi.org/10.1021/bi500724k | *Biochemistry* 2014, 53, 5280−5289

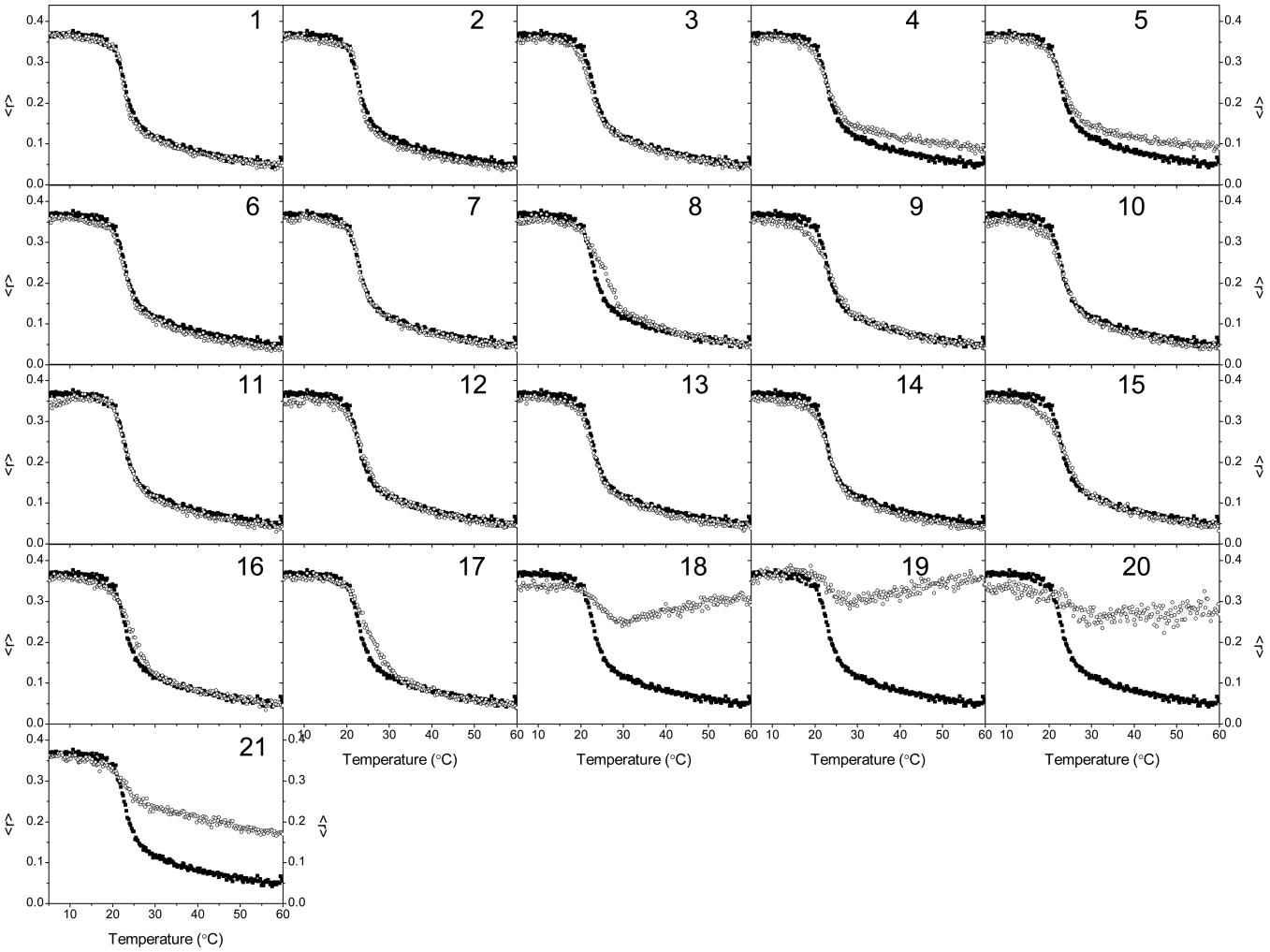

Figure 5. Steady-state anisotropy, ⟨*r*⟩, of the DPH probe incorporated into DMPG model membranes as a function of temperature in the presence of the peptide library corresponding to prM at pH 7.4. Each peptide is identified by its corresponding number. Data correspond to vesicles containing pure phospholipid (●) and phospholipid and peptide (○). The peptide:phospholipid molar ratio was 1:15.

transmembrane regions of the prM protein, with the deep part of the membrane (the DPH probe is known to be located inside the palisade structure of the membrane).

In conclusion, using both theoretical and experimental data, we have been able to identify different protein−protein and protein−membrane interacting regions on the DENV prM protein, highlighting the fact that the pr moiety could interact with the fusion E protein and with the M moiety (Figure 3 of the Supporting Information). Apart from the two transmembrane regions of prM (regions 5 and 6, Figure 3), the most relevant interacting regions should be regions 1 (protein−protein, pr domain) and 4 (membrane−protein, M domain). It should be recalled that the E protein also possesses several membrane interacting domains apart from two proposed transmembrane ones.[28] Our data would imply that the prM protein could be engaged in both protein−protein and lipid−protein interactions thorough the different regions described in this work, which might help us to understand its specific role in the DENV viral cycle. Apart from that, the M moiety could interact with the membrane interface through the stem/interfacial segment of the protein, modifying the ability of the E protein to interact with it. From the general picture shown above, it can be gathered that the distribution of interfaciality and hydrophobicity on the protein surface would relate to its biological function, i.e., membrane traversing segments, membrane surface interaction, protein−protein oligomerization, and/or protein−protein interaction. Furthermore, it is known that viral proteins can interconvert between different structures with different biological properties (active vs inactive and mature vs immature states). These structural transitions are driven by a plethora of molecular interactions, including interactions between membranotropic protein segments such as those described here, an indication of the significance of highlighting and characterizing them.

■ CONCLUSIONS

We have identified different regions of the DENV prM protein highlighting that the pr moiety could interact with the fusion E protein and with the M moiety. The pr moiety would comprise two segments, membrane and protein interacting domains, whereas the M moiety would comprise four segments, membrane and protein interacting domains as well as two transmembrane domains. Apart from that, the M moiety could interact with the membrane interface through the stem/interfacial segment of the protein modifying the ability of the E protein to interact with it. These zones should be involved in a complex web of interactions with both the fusion E protein and

dx.doi.org/10.1021/bi500724k | *Biochemistry* 2014, 53, 5280−5289

the membrane and should be considered interesting therapeutic targets.

■ ASSOCIATED CONTENT

Supporting Information

Two figures displaying the steady-state anisotropy of the DPH probe incorporated into DMPC model membranes in the presence of the peptide library corresponding to prM at pH 7.4 and 6.0. This material is available free of charge via the Internet at http://pubs.acs.org.

■ AUTHOR INFORMATION

Corresponding Author

*Instituto de Biología Molecular y Celular, Universidad "Miguel Hernández", E-03202 Alicante, Spain. Telephone: +34 966 658 762. Fax: +34 966 658 758. E-mail: jvillalain@umh.es.

Funding

This work was partially supported by Grant BFU2008-02617-BMC (Ministerio de Ciencia y Tecnología, Spain) to J.V. H.N. is supported by a FPU fellowship from MECD (Ministerio de Educación, Cultura y Deporte), Spain.

Notes

The authors declare no competing financial interest.

■ ACKNOWLEDGMENTS

We are especially grateful to BEI Resources, National Institute of Allergy and Infectious Diseases, Manassas, VA, for the peptides used in this work.

■ ABBREVIATIONS

BPI, bovine liver L-α-phosphatidylinositol; BPS, bovine brain L-α-phosphatidylserine; CF, 5-carboxyfluorescein; CHOL, cholesterol; CL, bovine heart cardiolipin; DENV, Dengue virus; DMPC, 1,2-dimyristoyl-*sn*-glycero-3-phosphatidylcholine; DMPG, 1,2-dimyristoyl-*sn*-glycero-3-[phospho-*rac*-glycerol]; DPH, 1,6-diphenyl-1,3,5-hexatriene; DSC, differential scanning calorimetry; EPA, egg L-α-phosphatidic acid; EPC, egg L-α-phosphatidylcholine; ER, endoplasmic reticulum; ESM, egg sphingomyelin; LUVs, large unilamellar vesicles; MLVs, multilamellar vesicles; T_m, temperature of the gel to liquid-crystalline phase transition; TM, transmembrane domain; TPE, egg transphosphatidylated L-α-phosphatidylethanolamine.

■ REFERENCES

(1) Guzman, M. G., and Kouri, G. (2002) Dengue: An update. *Lancet Infect. Dis. 2*, 33−42.

(2) Halstead, S. B. (2007) Dengue. *Lancet 370*, 1644−1652.

(3) Mukhopadhyay, S., Kuhn, R. J., and Rossmann, M. G. (2005) A structural perspective of the flavivirus life cycle. *Nat. Rev. Microbiol. 3*, 13−22.

(4) Bhatt, S., Gething, P. W., Brady, O. J., Messina, J. P., Farlow, A. W., Moyes, C. L., Drake, J. M., Brownstein, J. S., Hoen, A. G., Sankoh, O., Myers, M. F., George, D. B., Jaenisch, T., Wint, G. R., Simmons, C. P., Scott, T. W., Farrar, J. J., and Hay, S. I. (2013) The global distribution and burden of dengue. *Nature 496*, 504−507.

(5) World Health Organization (2009) *Dengue: Guidelines for Diagnosis, Treatment, Prevention and Control*, World Health Organization, Geneva.

(6) Pastorino, B., Nougairede, A., Wurtz, N., Gould, E., and de Lamballerie, X. (2010) Role of host cell factors in flavivirus infection: Implications for pathogenesis and development of antiviral drugs. *Antiviral Res. 87*, 281−294.

(7) Perera, R., and Kuhn, R. J. (2008) Structural proteomics of dengue virus. *Curr. Opin. Microbiol. 11*, 369−377.

(8) Bressanelli, S., Stiasny, K., Allison, S. L., Stura, E. A., Duquerroy, S., Lescar, J., Heinz, F. X., and Rey, F. A. (2004) Structure of a flavivirus envelope glycoprotein in its low-pH-induced membrane fusion conformation. *EMBO J. 23*, 728−738.

(9) Kielian, M., and Rey, F. A. (2006) Virus membrane-fusion proteins: More than one way to make a hairpin. *Nat. Rev. Microbiol. 4*, 67−76.

(10) Miller, S., Kastner, S., Krijnse-Locker, J., Buhler, S., and Bartenschlager, R. (2007) The non-structural protein 4A of dengue virus is an integral membrane protein inducing membrane alterations in a 2K-regulated manner. *J. Biol. Chem. 282*, 8873−8882.

(11) Miller, S., and Krijnse-Locker, J. (2008) Modification of intracellular membrane structures for virus replication. *Nat. Rev. Microbiol. 6*, 363−374.

(12) Welsch, S., Miller, S., Romero-Brey, I., Merz, A., Bleck, C. K., Walther, P., Fuller, S. D., Antony, C., Krijnse-Locker, J., and Bartenschlager, R. (2009) Composition and three-dimensional architecture of the dengue virus replication and assembly sites. *Cell Host Microbe 5*, 365−375.

(13) Qi, R. F., Zhang, L., and Chi, C. W. (2008) Biological characteristics of dengue virus and potential targets for drug design. *Acta Biochim. Biophys. Sin. 40*, 91−101.

(14) Hsieh, S. C., Zou, G., Tsai, W. Y., Qing, M., Chang, G. J., Shi, P. Y., and Wang, W. K. (2011) The C-terminal helical domain of dengue virus precursor membrane protein is involved in virus assembly and entry. *Virology 410*, 170−180.

(15) Li, L., Lok, S. M., Yu, I. M., Zhang, Y., Kuhn, R. J., Chen, J., and Rossmann, M. G. (2008) The flavivirus precursor membrane-envelope protein complex: Structure and maturation. *Science 319*, 1830−1834.

(16) Catteau, A., Kalinina, O., Wagner, M. C., Deubel, V., Courageot, M. P., and Despres, P. (2003) Dengue virus M protein contains a proapoptotic sequence referred to as ApoptoM. *J. Gen. Virol. 84*, 2781−2793.

(17) Brault, J. B., Kudelko, M., Vidalain, P. O., Tangy, F., Despres, P., and Pardigon, N. (2011) The interaction of flavivirus M protein with light chain Tctex-1 of human dynein plays a role in late stages of virus replication. *Virology 417*, 369−378.

(18) Duan, X., Lu, X., Li, J., and Liu, Y. (2008) Novel binding between pre-membrane protein and vacuolar ATPase is required for efficient dengue virus secretion. *Biochem. Biophys. Res. Commun. 373*, 319−324.

(19) Gao, F., Duan, X., Lu, X., Liu, Y., Zheng, L., Ding, Z., and Li, J. (2010) Novel binding between pre-membrane protein and claudin-1 is required for efficient dengue virus entry. *Biochem. Biophys. Res. Commun. 391*, 952−957.

(20) Che, P., Tang, H., and Li, Q. (2013) The interaction between claudin-1 and dengue viral prM/M protein for its entry. *Virology 446*, 303−313.

(21) Wong, S. S., Haqshenas, G., Gowans, E. J., and Mackenzie, J. (2012) The dengue virus M protein localises to the endoplasmic reticulum and forms oligomers. *FEBS Lett. 586*, 1032−1037.

(22) Halstead, S. B. (2013) Identifying protective dengue vaccines: Guide to mastering an empirical process. *Vaccine 31*, 4501−4507.

(23) Perez-Berna, A. J., Veiga, A. S., Castanho, M. A., and Villalain, J. (2008) Hepatitis C virus core protein binding to lipid membranes: The role of domains 1 and 2. *Journal of Viral Hepatitis 15*, 346−356.

(24) Guillen, J., Perez-Berna, A. J., Moreno, M. R., and Villalain, J. (2005) Identification of the membrane-active regions of the severe acute respiratory syndrome coronavirus spike membrane glycoprotein using a 16/18-mer peptide scan: Implications for the viral fusion mechanism. *J. Virol. 79*, 1743−1752.

(25) Perez-Berna, A. J., Moreno, M. R., Guillen, J., Bernabeu, A., and Villalain, J. (2006) The membrane-active regions of the hepatitis C virus E1 and E2 envelope glycoproteins. *Biochemistry 45*, 3755−3768.

(26) Moreno, M. R., Giudici, M., and Villalain, J. (2006) The membranotropic regions of the endo and ecto domains of HIV gp41 envelope glycoprotein. *Biochim. Biophys. Acta 1758*, 111−123.

(27) Perez-Berna, A. J., Guillen, J., Moreno, M. R., Bernabeu, A., Pabst, G., Laggner, P., and Villalain, J. (2008) Identification of the Membrane-active Regions of Hepatitis C Virus p7 Protein: Biophysical Characterization of the Loop Region. *J. Biol. Chem. 283*, 8089−8101.
(28) Nemesio, H., Palomares-Jerez, F., and Villalain, J. (2011) The membrane-active regions of the dengue virus proteins C and E. *Biochim. Biophys. Acta 1808*, 2390−2402.
(29) Keenan, T. W., and Morre, D. J. (1970) Phospholipid class and fatty acid composition of Golgi apparatus isolated from rat liver and comparison with other cell fractions. *Biochemistry 9*, 19−25.
(30) Krainev, A. G., Ferrington, D. A., Williams, T. D., Squier, T. C., and Bigelow, D. J. (1995) Adaptive changes in lipid composition of skeletal sarcoplasmic reticulum membranes associated with aging. *Biochim. Biophys. Acta 1235*, 406−418.
(31) Böttcher, C. S. F., Van Gent, C. M., and Fries, C. (1961) A rapid and sensitive sub-micro phosphorus determination. *Anal. Chim. Acta 1061*, 203−204.
(32) Edelhoch, H. (1967) Spectroscopic determination of tryptophan and tyrosine in proteins. *Biochemistry 6*, 1948−1954.
(33) Mayer, L. D., Hope, M. J., and Cullis, P. R. (1986) Vesicles of variable sizes produced by a rapid extrusion procedure. *Biochim. Biophys. Acta 858*, 161−168.
(34) Bernabeu, A., Guillen, J., Perez-Berna, A. J., Moreno, M. R., and Villalain, J. (2007) Structure of the C-terminal domain of the pro-apoptotic protein Hrk and its interaction with model membranes. *Biochim. Biophys. Acta 1768*, 1659−1670.
(35) Moreno, M. R., Guillen, J., Perez-Berna, A. J., Amoros, D., Gomez, A. I., Bernabeu, A., and Villalain, J. (2007) Characterization of the Interaction of Two Peptides from the N Terminus of the NHR Domain of HIV-1 gp41 with Phospholipid Membranes. *Biochemistry 46*, 10572−10584.
(36) Lentz, B. R. (1993) Use of fluorescent probes to monitor molecular order and motions within liposome bilayers. *Chem. Phys. Lipids 64*, 99−116.
(37) Guillen, J., Gonzalez-Alvarez, A., and Villalain, J. (2010) A membranotropic region in the C-terminal domain of hepatitis C virus protein NS4B interaction with membranes. *Biochim. Biophys. Acta 1798*, 327−337.
(38) Palomares-Jerez, M. F., and Villalain, J. (2011) Membrane interaction of segment H1 (NS4B(H1)) from hepatitis C virus non-structural protein 4B. *Biochim. Biophys. Acta 1808*, 1219−1229.
(39) Gadkari, R. A., and Srinivasan, N. (2010) Prediction of protein-protein interactions in dengue virus coat proteins guided by low resolution cryoEM structures. *BMC Struct. Biol. 10*, 17.
(40) Palomares-Jerez, F., Nemesio, H., and Villalain, J. (2012) The membrane spanning domains of protein NS4B from hepatitis C virus. *Biochim. Biophys. Acta 1818*, 2958−2966.
(41) Nemesio, H., Palomares-Jerez, F., and Villalain, J. (2012) NS4A and NS4B proteins from dengue virus: Membranotropic regions. *Biochim. Biophys. Acta 1818*, 2818−2830.
(42) White, S. H., and Wimley, W. C. (1999) Membrane protein folding and stability: Physical principles. *Annu. Rev. Biophys. Biomol. Struct. 28*, 319−365.
(43) Engelman, D. M., Steitz, T. A., and Goldman, A. (1986) Identifying nonpolar transbilayer helices in amino acid sequences of membrane proteins. *Annu. Rev. Biophys. Biophys. Chem. 15*, 321−353.
(44) Hessa, T., Meindl-Beinker, N. M., Bernsel, A., Kim, H., Sato, Y., Lerch-Bader, M., Nilsson, I., White, S. H., and von Heijne, G. (2007) Molecular code for transmembrane-helix recognition by the Sec61 translocon. *Nature 450*, 1026−1030.
(45) Moon, C. P., and Fleming, K. G. (2011) Side-chain hydrophobicity scale derived from transmembrane protein folding into lipid bilayers. *Proc. Natl. Acad. Sci. U.S.A. 108*, 10174−10177.
(46) Koehler, J., Woetzel, N., Staritzbichler, R., Sanders, C. R., and Meiler, J. (2009) A unified hydrophobicity scale for multispan membrane proteins. *Proteins 76*, 13−29.
(47) Eisenberg, D., Weiss, R. M., and Terwilliger, T. C. (1982) The helical hydrophobic moment: A measure of the amphiphilicity of a helix. *Nature 299*, 371−374.